

THE IMPACT OF A FILAMENT ERUPTION ON NEARBY HIGH-LYING COOL LOOPS

L. K. HARRA¹, S. A. MATTHEWS¹, D. M. LONG¹, G. A. DOSCHEK², AND B. DE PONTIEU³

¹ UCL-Mullard Space Science Laboratory, Holmbury St Mary, Dorking, Surrey, RH5 6NT, UK; l.harra@ucl.ac.uk

² Space Science Division, Naval Research Laboratory, Washington, DC 20375, USA

³ Lockheed Martin Solar and Astrophysics Laboratory, Org. A021S, Building 252, 3251 Hanover Street, Palo Alto, CA 94304, USA

Received 2014 May 29; accepted 2014 July 16; published 2014 August 20

ABSTRACT

The first spectroscopic observations of cool Mg II loops above the solar limb observed by NASA’s Interface Region Imaging Spectrograph (IRIS) are presented. During the observation period, IRIS is pointed off-limb, allowing the observation of high-lying loops, which reach over 70 Mm in height. Low-lying cool loops were observed by the IRIS slit-jaw camera for the entire four-hour observing window. There is no evidence of a central reversal in the line profiles, and the Mg II h/k ratio is approximately two. The Mg II spectral lines show evidence of complex dynamics in the loops with Doppler velocities reaching ± 40 km s⁻¹. The complex motions seen indicate the presence of multiple threads in the loops and separate blobs. Toward the end of the observing period, a filament eruption occurs that forms the core of a coronal mass ejection. As the filament erupts, it impacts these high-lying loops, temporarily impeding these complex flows, most likely due to compression. This causes the plasma motions in the loops to become blueshifted and then redshifted. The plasma motions are seen before the loops themselves start to oscillate as they reach equilibrium following the impact. The ratio of the Mg h/k lines also increases following the impact of the filament.

Key words: Sun: chromosphere – Sun: corona – Sun: coronal mass ejections (CMEs)

Online-only material: animations, color figures

1. INTRODUCTION

Cool loops have been observed in non-flaring active regions and in post-flare loop systems for many years. Complex motions are often seen in loops when the plasma cools, a phenomenon that is sometimes described as “coronal rain.” These have been observed for many decades (e.g., Kawaguchi 1970). More recently, Schrijver (2001) analyzed data from the *Transition Region and Coronal Explorer (TRACE)* spacecraft and found that coronal rain in active regions was observed approximately every two days. Recent high-resolution observations with *Hinode*, NASA’s *Solar Dynamics Observatory (SDO)* (Lemen et al. (2012)), and instruments such as CRISP on the Swedish Solar Telescope have shown the coronal rain to consist of small and dense chromospheric cores with falling speeds of tens of km s⁻¹ (Antolin & Rouppe Van Der Voort 2012). In these higher-resolution data sets, the rain appears to be ubiquitous, and it has been suggested that the Schrijver (2001) observations with *TRACE* may have been picking up time periods when the blobs occur close together and in large quantities, in what is sometimes called a “shower.” A range of speeds have been observed for the rain, reaching a peak of 120 km s⁻¹, but with an average speed of around 60 km s⁻¹. Coronal rain can be most easily seen at the limb, but has been observed on the disk by Antolin et al. (2012). The small-scale features of the rain are important to understand as their descent may follow the magnetic field lines and thus can provide information about the magnetic field structure. The rain is usually observed in chromospheric lines such as H α and Ca II H and in absorption in EUV spectral lines. However, sources that resemble coronal rain have even been observed in white light during solar flares (Martinez Oliveros et al. 2014). One interpretation for coronal rain is that hot loops will rapidly cool down through thermal conduction and radiation until becoming thermally unstable. This leads to the formation of the blob-like condensations.

Spectral line profiles of Mg II have rarely been measured above the limb. Skylab data were analyzed (Feldman and Doschek 1977) in the quiet Sun and an active region, and it was found that above 8” the central reversal seen in the Mg II lines on the disk disappears. A quiescent prominence was also observed in Mg II by the OSO-8 spacecraft (Vial et al. 1981), and blueshifts were found, reaching around 14 km s⁻¹.

In this paper, we study cool loops observed by Interface Region Imaging Spectrograph (IRIS) on the 2013 October 26. IRIS is pointing off-limb, and hence allows us to explore the behavior of cool loops lying above 30 Mm in height. These are the first observations of Mg II spectra at these altitudes. During the time of this observation, a filament eruption occurs that disrupts these high-lying loops. We analyze the cool loops using the slit-jaw data from IRIS together with spectroscopic measurement of Mg II before the eruption and discuss the changes that occur as the eruption impacts these preexisting loops. This is the first time that the impact of a filament eruption has been observed spectroscopically in these high-lying cool loops.

2. OBSERVATIONS

We made use of data sets from *SDO*, Lemen et al. (2012), and IRIS. *SDO* provides images of the full Sun in multiple passbands revealing the behavior of plasma at different temperatures. Figure 1 shows the AIA 304 Å light curve which indicates the activity levels of the filament as it erupts. This figure also indicates when cool loops were lying at high enough altitudes to be seen in the IRIS field of view. IRIS (De Pontieu et al. 2014) provides simultaneous spectra and images of the photosphere, chromosphere, transition region, and corona with 0.33–0.4 arcsec spatial resolution, two-second temporal resolution, and 1 km s⁻¹ velocity resolution over a field of view of up to 175 arcsec \times 175 arcsec. IRIS was launched into a Sun-synchronous orbit on 2013 June 27. The bandpasses include spectral lines

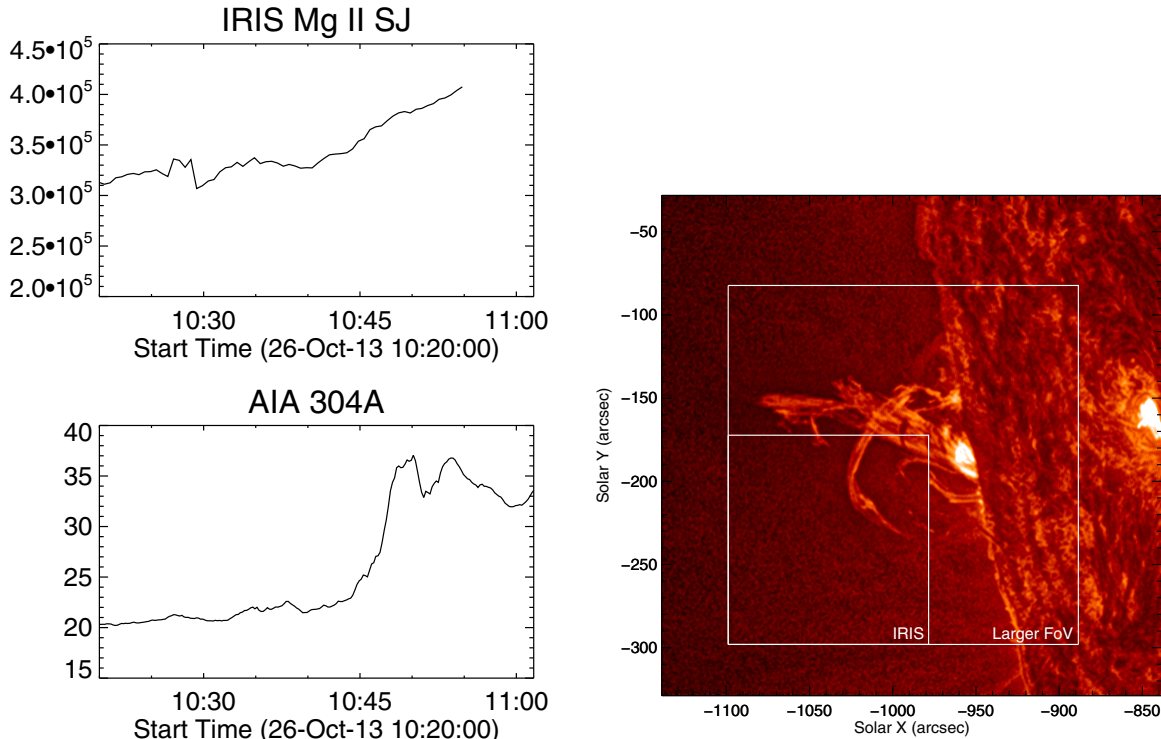


Figure 1. Right: an *SDO* AIA image focused on the active region at the limb. Left: light curve from AIA 304 Å passband from the larger FOV (lower plot) and light curve of the IRIS Mg II slit-jaw data (top plot). The animation shows the AIA 304 Å movie along with the IRIS Mg II movie.

(An animation and a color version of this figure are available in the online journal.)

formed in the chromosphere (Mg II h 2803 and Mg II k 2796) and transition region (C II 1334/1335 and Si IV 1394/1403). Slit-jaw images are taken simultaneously. In our observations, the slit-jaw camera observes from ≈ 35 Mm, and the slit observed at ≈ 70 Mm above the limb. From Movie 1, it is clearly seen that there are cool loops during the whole observing time that lie below an altitude of 30 Mm. We analyze the time period from 10:20–10:54 UT, which shows newly formed high-lying loops that are subsequently impacted by a filament eruption. Due to the high altitude of the observed loops, the count rates are very low in the C II, Si IV, and Fe XII spectral lines, so we focused our analysis on the strong Mg II lines. The analysis was carried out with the level 2 data files as recommended in the IRIS data analysis guide. For the determination of the Doppler velocity, we took an average of the spectrum along the slit. This gave us a rest wavelength of 2796.6 Å. This is close to the National Institute of Standard and Technology wavelength in a vacuum for Mg II k of 2796.35 Å. The central reversal appears to have disappeared in the line profiles, consistent with earlier observations of this emission above the limb, indicating that the plasma is optically thin. This can be seen clearly in the spectra of the “isolated” blob in Figure 2, which is described in the next section.

2.1. Characterizing a Single Blob

The structure of the cool loops is very complex—there are multiple strands with a “loop” structure, while at other times isolated blobs appear to follow the track of a magnetic loop. To explore the behavior of the structures, we first isolate a single cool blob as it falls. Figure 2 shows an isolated blob of cool plasma falling downward highlighted with the black line. The blob was tracked, and plasma flows were measured from the

slit-jaw images. There is a clear propagation along the black line, and the speed of the blob falling in the plane of the sky was measured to be ≈ 34 km s $^{-1}$. Figure 2 also shows the Mg II spectrum at the time the blob appears crosses the IRIS slit. The plot on the left shows this motion as a function of y -slit position and wavelength, while the right plot shows a sample spectrum. The spectrum is a simple Gaussian, with no evidence of multiple components and no evidence of central reversal of the lines. It is redshifted with a speed of ≈ 15 km s $^{-1}$. If we look at both the h and k lines, the ratio of the integrated spectral line intensities is 1.55. The ratio of the oscillator strengths of the h and k lines for simple electron impact excitation should be 2:1—and for radiation, it should be 4:1. In this example, the ratio is less than two (Figure 3), which suggests that radiative effects should be minimal, but may indicate the presence of resonance scattering. Values such as this have been observed before, for example, with Skylab data by Doschek et al. (1977), where values have been found that are 1.5 at 2'' above the solar limb. More recent work by Keenan et al. (2014) has shown for the first time that in the solar case, this ratio can change in both directions as the result of opacity.

This example was a rare isolated blob of short duration. The longer-lasting loop structures show much more complexity in the brightness structures and flows, which suggests that they may be composed of multiple component loops and falling blobs that are lying at slightly different angles to each other; hence, the cool plasma falls at different orientations, each providing a different component to the Mg II profiles when the loops are so close together. This is suggestive of braiding, which was predicted theoretically by Parker (1983). Braiding has been seen both in the chromosphere (Martin 1998) and, more recently, in the corona (Cirtain et al. 2013). We discuss the temporal evolution of the more complex structure in the next section, and we describe

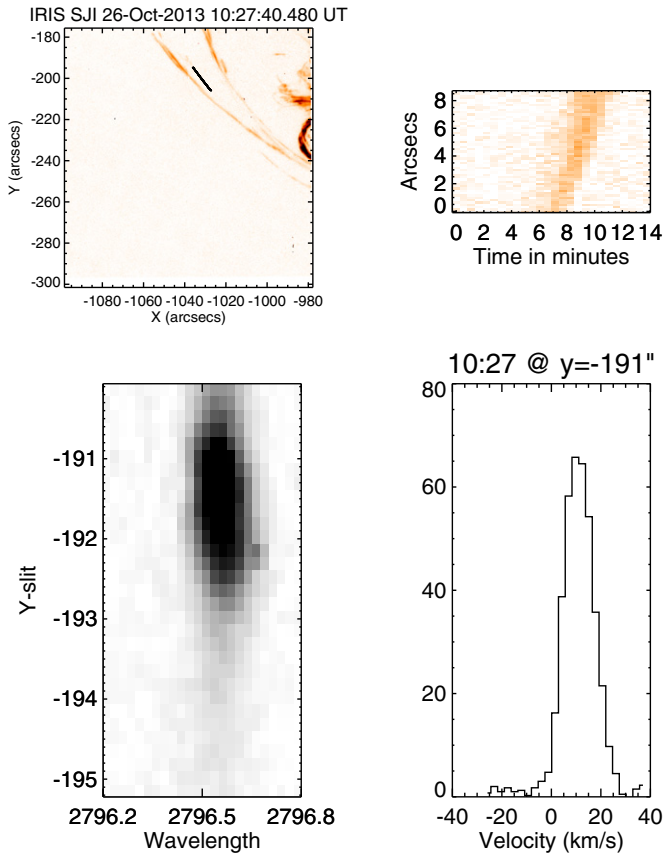


Figure 2. Top left: the slit-jaw image in Mg II. The black line highlights a blob of falling, cool plasma that we studied. Top right: the motion of the blob (zero arcseconds is the top of the black line). There is a clear propagation along this line with a speed of around 34 km s^{-1} . Bottom left: the spectra of Mg II along the slit as the blob falls downward. Bottom right: sample spectra at 10:27 at the y position 191 arcsec.

(A color version of this figure is available in the online journal.)

how the filament eruption changes the plasma behavior in the loops.

2.2. Temporal Evolution of the Plasma in the High-lying Loops Before and During the Filament Impact

Figure 4 shows example images from the IRIS slit-jaw camera of the $10\text{--}20 \times 10^3 \text{ K}$ Mg II and coronal AIA 171 \AA plasma. These images also show the location of the slit during this observation. The right-hand panels of Figure 4 show a stack plot image of the Mg II k slit data with time where the slit crosses the cool loops. The loops seen are extremely dynamic showing fine structures and blob-like features falling continuously toward the solar disk as the loops cool (see Movie 1). The loops appear to provide pathways for the cooling plasma to rain down into the lower solar atmosphere. This complex structure stays at the same location for a long time (more than 10 minutes) centered at $-199''$. At around 10:48 UT, the loops are moved in a southward direction, which can be seen in the lower right stack plot that shows a downward turning with speeds around 30 km s^{-1} . Figure 4 also shows the AIA 171 \AA data with a simulated stack plot in the same location. The IRIS observations of this region unfortunately stop at 10:54 UT before the loops have reached an equilibrium following the disruption. However, the AIA 171 \AA data clearly shows how the loops recover with some oscillatory motion afterward. These loop oscillations are known

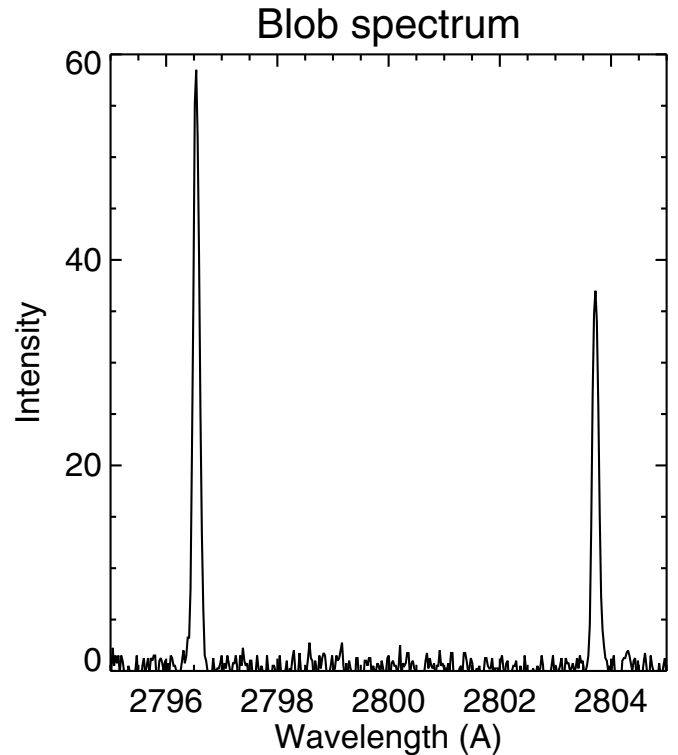


Figure 3. Sample spectrum of the Mg II h and k lines in the isolated blob. The line intensity ratio of the two lines is 1.55. There is no evidence of central reversal in these lines.

to be triggered by a nearby flare or eruption (e.g., Nakariakov et al. 1999).

Figure 5 shows IRIS data from the slit-jaw camera on the left and Mg II k spectral profiles on the right at four different times. The top images show the newly formed high-lying loops, and the next three images show the time period when the filament eruption impacted the loops. Movie 2 shows how the spectra change with time during the whole observing period. The Mg II slit-jaw images show the fine structure of the loops above the limb. However, the velocity scale indicates that speeds of $\approx 40 \text{ km s}^{-1}$ blueshifted (toward Earth) and $\approx 40 \text{ km s}^{-1}$ redshifted (away from the Earth) are present at different times. In the first image showing the “quiescent” cool loops, the structure is complex, with multiple “layers” of threads, and there is evidence of more than one component in the spectral lines at times. The complexity of the loop structure, including the falling blobs, is reminiscent of the coronal rain observed by Antolin & Rouppe Van Der Voort (2012) where redshifted and blueshifted velocities of the same magnitude ($\approx 40 \text{ km s}^{-1}$) were observed in the $H\alpha$ line.

The filament eruption is first seen in the IRIS field of view at 10:45 UT in the top right-hand part of the image in Figure 5 as a high-intensity feature (clearly seen in Movie 1). At 10:52 UT, this is more prominent. The high-lying loops are impacted before this cool filamentary material reaches it, indicating that we do not see the front of the eruption at these cool temperatures. The sample spectrum at 10:50 UT shows the initial change that happens following the eruption impacting these loops. The spectra at this stage have narrower and less complex profiles, which indicate that some of the dynamics have been inhibited. At 10:52, the profiles show a significant change, now becoming predominantly blueshifted. At 10:54, this has changed again

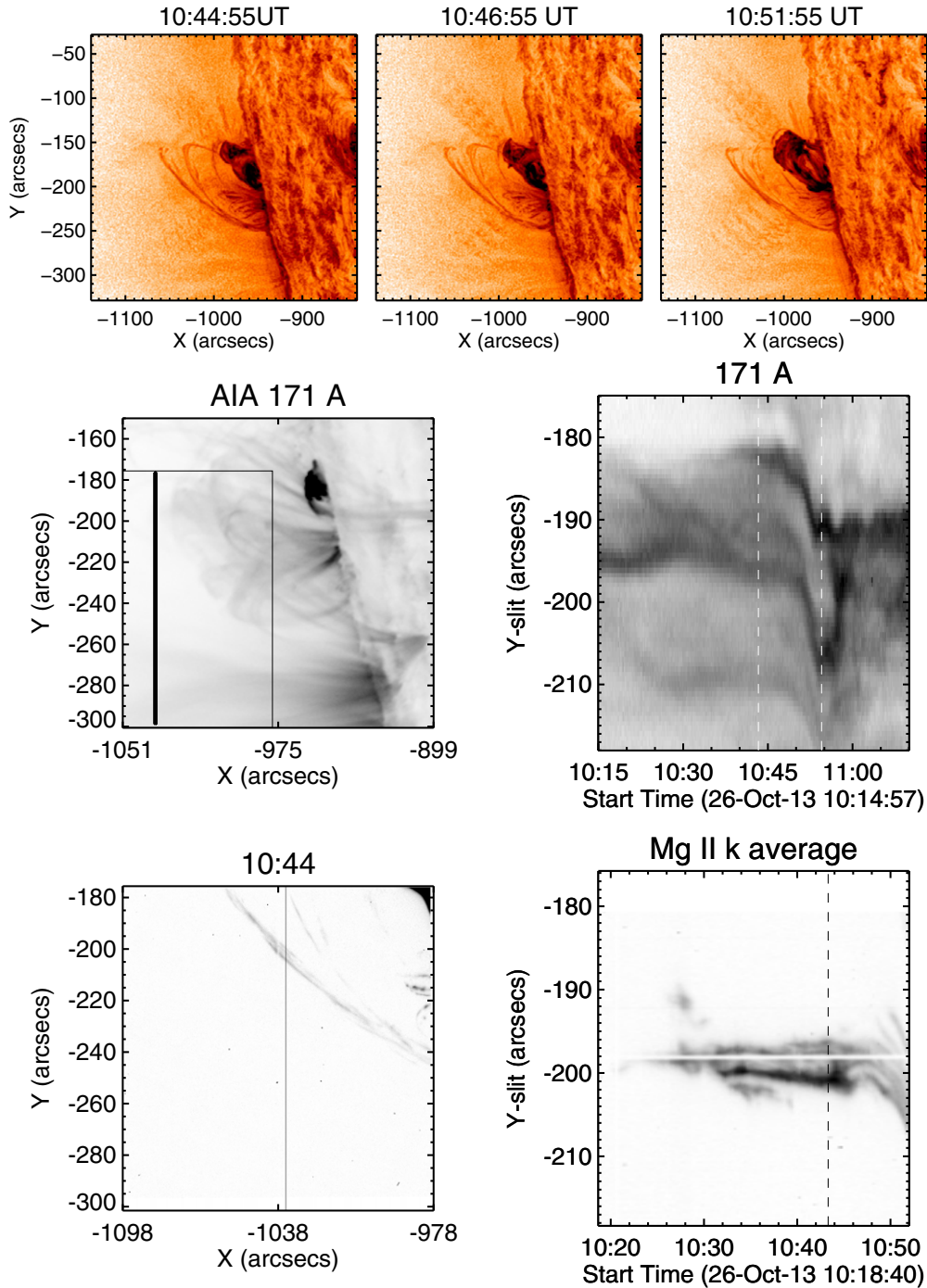


Figure 4. Top three panels present AIA 304 Å data showing the filament eruption starting. The middle left panel shows a 171 Å AIA image with the IRIS field of view highlighted by a black box. The thick vertical black line shows the position where the AIA stack plot was made. The middle right panel shows the AIA stack plot. The first white vertical lines highlight the start of the eruption, and the second vertical lines indicate the end of the IRIS observations. Please note the y axis has been changed to focus in on the dynamic features. The bottom left panel presents the IRIS slit-jaw image at 2796 Å showing the loops lying high in the corona. The black vertical line shows where the slit is located. The bottom right panel shows the IRIS slit data with time. The spectra have been integrated over wavelength to yield intensities. Distinct and broad features exist that appear to consist of many loops. Initially the loops are seen lying at roughly the same location, but moving dynamically (at around $-200''$), just before 10:50 UT the eruption propagates through and pushes the loops downward by nearly $10''$ with a speed of 30 km s^{-1} . (A color version of this figure is available in the online journal.)

with the profiles showing redshifts. These significant changes in the plasma dynamics are all occurring when the loops are still moving due to the eruption. Movie 2 shows the IRIS Mg II k profile with time along the slit.

In order to appreciate the intricacy of the flows during this period, we fitted each spectrum with a two-component fit.

The spectra are complex, and several component fits were attempted, with the two-component fit providing the best fit for the spectra. Figure 6 shows the intensity, Doppler velocity, and line width results for the main component of the spectra. When these high loops initially form around 10:25 UT, they are already showing flows (mostly redshifts). As time progresses

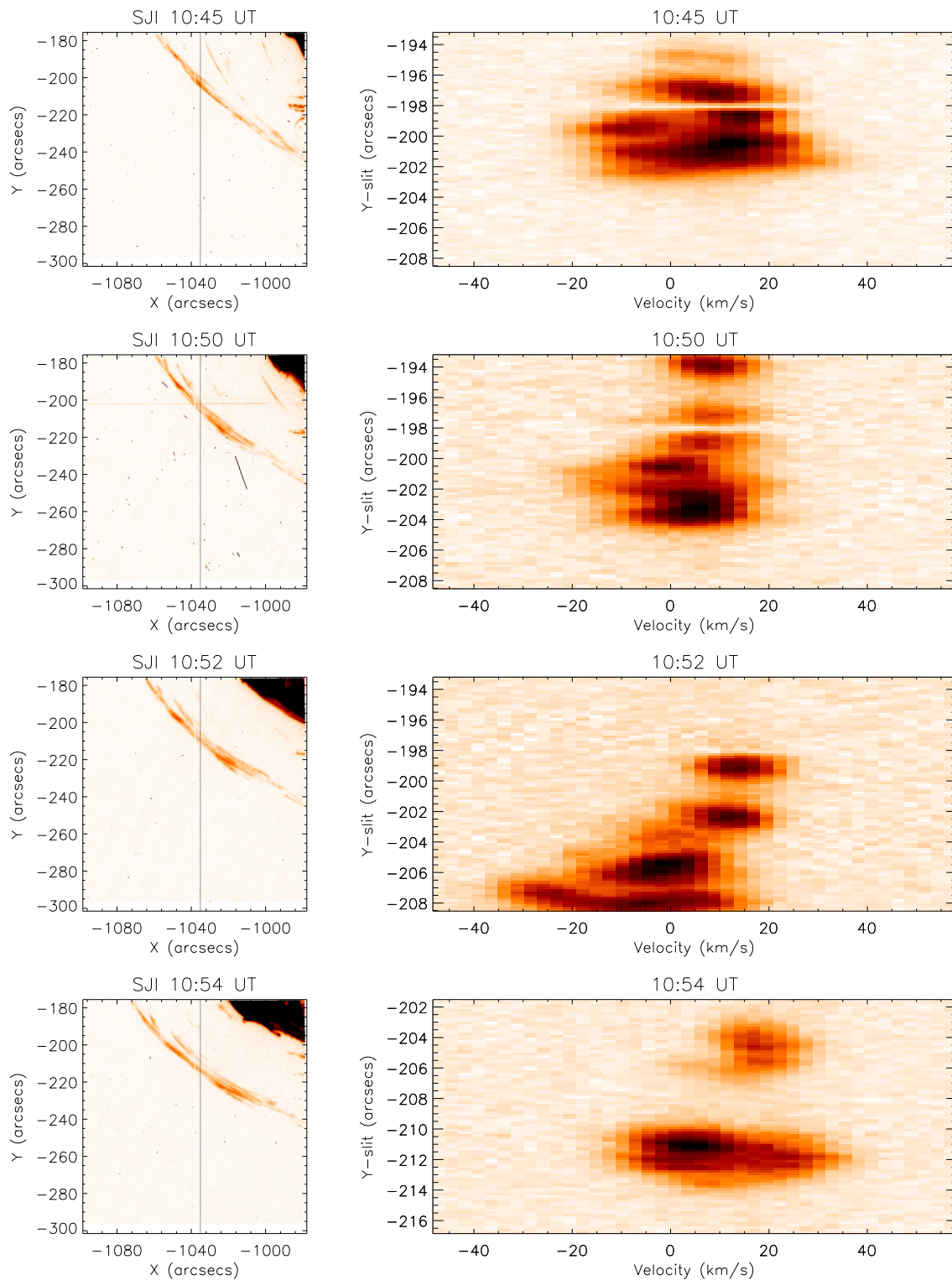


Figure 5. In the left-hand column, the IRIS slit-jaw images in 2796 \AA are shown at 10:45 UT, then at 10:50 UT (when the eruption begins to push the loops), at 10:52 UT, and at 10:54 UT. In the images, the cool material that forms the core of the eruption is seen at the top right of the image. The hotter front is not seen at these wavelengths. The right-hand column shows sample spectra of Mg II along the slit at each time. The spectra shown on the top right are at the same times as the images. The plasma in the loops show multiple features. At 10:50, once the eruption pushes the loops, the spectra are less complex with narrower line profiles, indicating simpler dynamics. At 10:52, the plasma shows a strong blueshift, and at 10:54, the plasma then becomes redshifted (please note that the y axis has changed in order to track this feature). These strong flows are seen while the loops are being pushed downward. The animation shows the spectra changing with time following the eruption. (An animation and a color version of this figure are available in the online journal.)

and more loops are created at these latitudes, there is a mix of redshifts and blueshifts. As the filament starts to impact the loops, there is an enhancement in line width (which indicates stronger flows in both directions) followed by a reduction in

both line width and Doppler flows. The plasma then becomes redshifted, blueshifted, and then redshifted again. The plasma is reorganizing itself parallel to the line of sight before there is any evidence of the “standard” loop displacements that have been

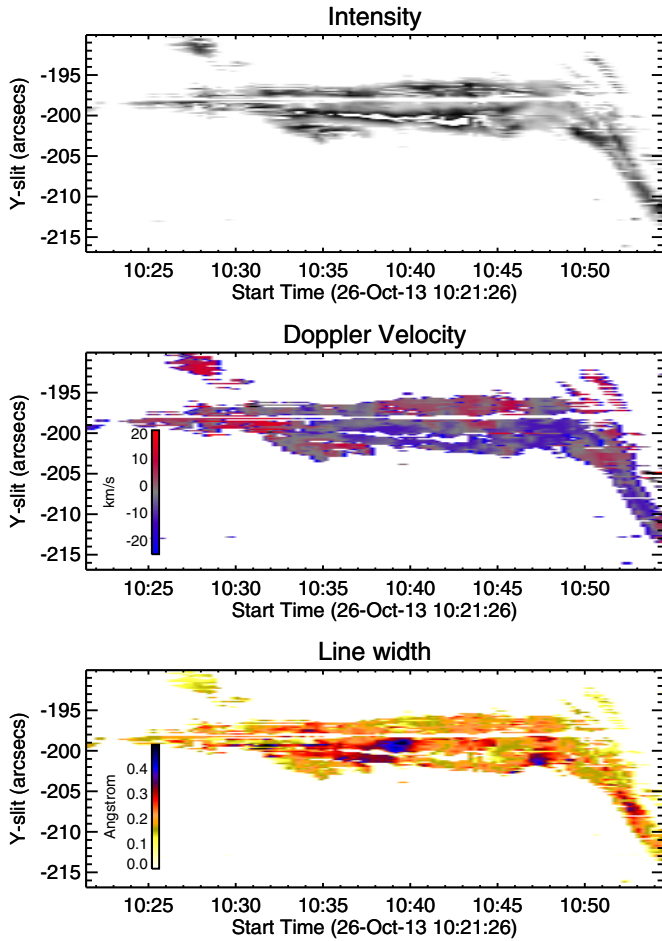


Figure 6. Two-component fit applied for the Mg II data. These figures show the Mg II slit data with time for the main fitted component—intensity is shown in the top panel, Doppler velocity in the middle panel, and line width in the bottom panel.

(A color version of this figure is available in the online journal.)

observed following eruptions (Nakariakov et al. (1999)). This is the first time this has been observed.

We determine the Mg II h/k ratio along the slit with time to determine if this changes during the impact of the filament. Examples of the Mg II h and k spectral lines are shown in Figure 7 spatially located in the center of the loop structure. At 10:35 UT before the filament eruption, the profiles shown no central reversal. In addition, the spectra are non-Gaussian broadened profiles compared with the spectrum of the isolated blob (Figure 2). There is evidence of a red-wing component. The ratio of the h/k line at this time is 1.5—similar to that of the isolated blob. At 10:50 UT just as the filament impacts these loops, the profiles again show complexity with stronger blue-wing components. The ratio of this stage has increased to 1.9. To show the temporal and spatial evolution of the intensity ratio, we determine this value in all the pixels that have statistically significant intensity values. Figure 8 shows the stack plot of the ratio. Most of the pixels have a ratio around 1.6 before the filament impacts. The ratio increases to two and above following the impact. At no stage does the ratio reach a value of four, which would indicate that radiation is the dominant process.

We are seeing significant changes in these high-lying loops following the impact of the filament—both in terms of the complex dynamics within the loops and in terms of the line intensity ratios.

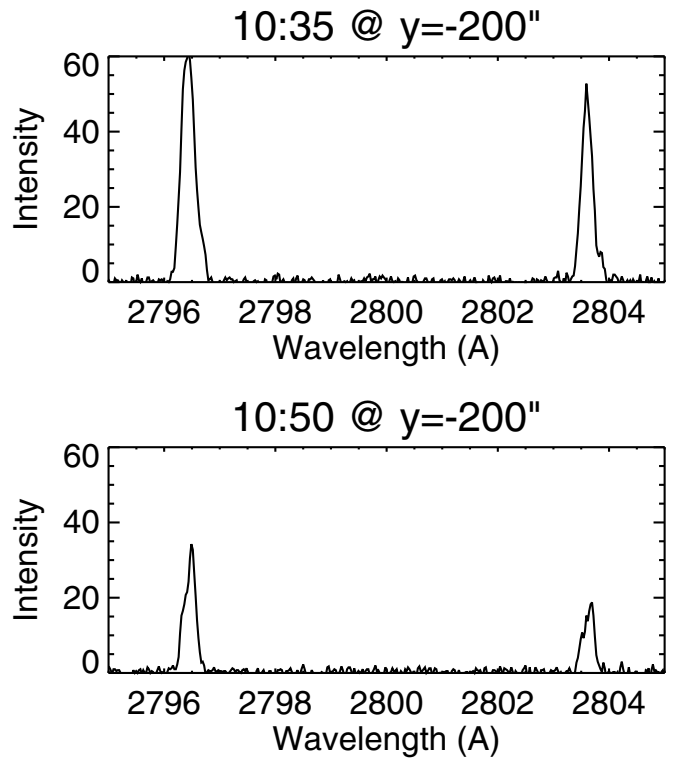


Figure 7. Sample Mg II spectra at $y = -200''$ before the filament eruption (top) and after the filament eruption (bottom).

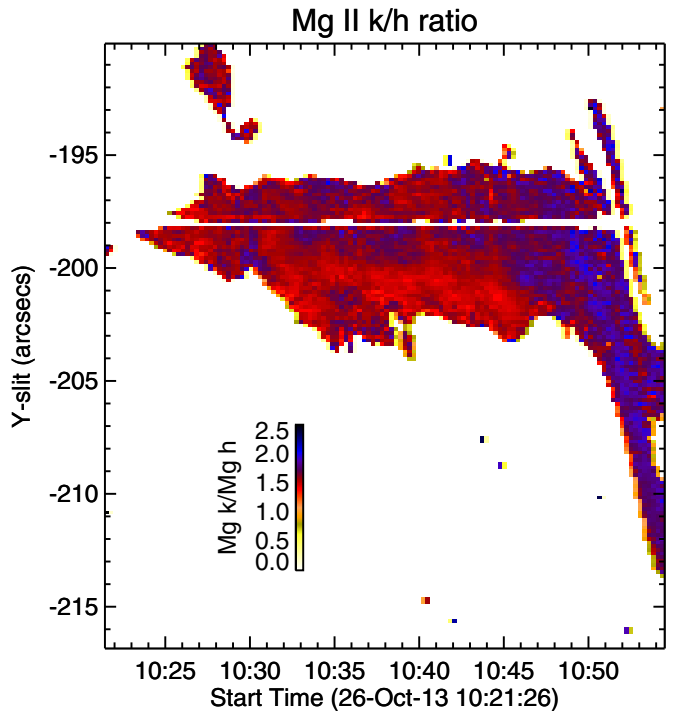


Figure 8. Stack plot of the Mg k/h ratio.

(A color version of this figure is available in the online journal.)

3. DISCUSSION

These observations show coronal rain above the limb observed for the first time in Mg II by the IRIS spacecraft. The line profiles show that the central reversal is gone. The complexity seen in the spectral lines can then be assumed to be

due to dynamics only. The spectral lines often show multiple components. We could in one instance isolate a blob of cool plasma falling, and we found that its spectral profile was close to a single Gaussian, suggesting that in the other cases there were multiple threads overlaid in the same field of view, within the spatial resolution of IRIS. The ratio of the h/k lines is around two and shows variation with time and space. These loops then experienced the impact of a large eruption. As the eruption propagates, it impacts the existing cool loops. The eruption has a cool filamentary core that is seen by IRIS, but the erupting plasma that initially reaches the cool loops is hotter and is not seen by IRIS. As the eruption impacts these loops, the complexity of the flows is temporarily reduced, most likely due to compression of the loops. Then the plasma is redshifted, blueshifted, and then redshifted again. Alongside this, the line intensity ratio of h/k increases during the impact, reaching above 2:1. It is possible that for this scenario, as the ratio becomes greater than 2:1, this might imply some additional radiative excitation along with the collisional excitation. The source of the radiative excitation above the limb may be enhanced by the flare and coronal mass ejection. Currently, there are no simulations that make observational predictions of the response of these high-lying loops during the impact of the eruption, and these observations provide important constraints for future modeling work in this area.

The IRIS data provide a microscope to the plasma dynamics of these cool high-lying loops during the filament eruption. From the images, we see clearly the loops disrupted by the filament eruption. In addition, IRIS demonstrates that the plasma inside reacts significantly to this event with the plasma reorganizing itself before intensity oscillations occur. The level of turbulence going on inside loops during such a process has not been observed before and allows us to probe plasma during a major disruption.

Hinode is a Japanese mission developed and launched by ISAS/JAXA, with NAOJ as domestic partner and NASA and STFC (UK) as international partners. It is operated by these agencies in cooperation with ESA and NSC (Norway). IRIS is a NASA small explorer mission developed and operated by LMSAL, with mission operations executed at NASA Ames Research center and major contributions to downlink communications funded by the Norwegian Space Center (NSC, Norway) through an ESA PRODEX contract. We thank the IRIS team for access to the data. The *Solar Dynamics Observatory* is a NASA mission. Data supplied courtesy of the *SDO/AIA* consortia. *SDO* is the first mission to be launched for NASA's Living With a Star (LWS) program. The research leading to these results has received funding from the European Commission's Seventh Framework Programme under grant agreement No. 284461 (eHEROES project). G.A.D. is supported by a *Hinode* grant from NASA.

REFERENCES

- Antolin, P., & Rouppe Van Der Voort, L. 2012, *ApJ*, **745**, 152
 Antolin, P., Vissers, G., & Rouppe Van Der Voort, L. 2012, *SoPh*, **280**, 457
 Cirtain, J., Golub, L., Winebarger, A. R., et al. 2013, *Natur*, **493**, 501
 De Pontieu, B., Title, A. M., Lemen, J. R., et al. 2014, *SoPh*, **289**, 2733
 Feldman, U., & Doschek, G. A. 1977, *ApJ*, **212**, 147
 Howard, R. A., Moses, J. D., Vourlidas, A., et al. 2008, *SSRv*, **136**, 67
 Kawaguchi, I. 1970, *PASJ*, **22**, 405
 Keenan, F. P., Doyle, J. G., Madjarska, M., et al. 2014, *ApJ*, **784**, 39
 Lemen, J. R., Title, A. M., Akin, D. J., et al. 2012, *SoPh*, **275**, 17
 Martin, S. 1998, *SoPh*, **182**, 107
 Martínez Oliveros, J.-C., Krucker, S., Hudson, H. S., et al. 2014, *ApJ*, **780**, 28
 Nakariakov, V., Ofman, L., DeLuca, E. E., et al. 1999, *Sci*, **285**, 862
 Parker, E. 1983, *ApJ*, **264**, 642
 Schrijver, C. J. 2001, *SoPh*, **198**, 325
 Vial, J. C., Salm-Platzer, J., & Matres, M. J. 1981, *SoPh*, **70**, 325